Electronic Supplementary Information

S Santhoshkumar,[1] Yan-Ru Liu[1], and Wei-Lung Tseng*[1,2]

[1]Department of Chemistry, National Sun Yat-sen University, No. 70 Lienhai Rd., Kaohsiung, 80424, Taiwan

[2]School of Pharmacy, College of Pharmacy, Kaohsiung Medical University, No.100, Shiquan 1st Rd., 80708, Kaohsiung, Taiwan

Correspondence: Dr. Wei-Lung Tseng

E-mail: tsengwl@mail.nsysu.edu.tw

Fax: 011-886-7-5254644

Experimental Section

Determination of luminescence QY. The luminescence QYs of LYZ-stabilized Au_8 and Au_{25} clusters were determined using quinine sulfate (QY = 0.54 in 0.1 M H_2SO_4) and BSA–stabilized AuNCs (QY = 0.06) as reference standards. Absorbance was adjusted to 0.01–0.05 (intervals of 0.01), and QYs were calculated according to the following equation:

$$Q = Q_R \frac{m}{m_R} \cdot \frac{n^2}{n_R^2}$$

Herein, Q is the quantum yield of the sample, Q_R is the quantum yield of the reference, m and m_R are the slopes of the integrated fluorescence intensity versus absorbance plots for the sample and reference, respectively, and n and n_R are the refractive indices of the solvents (with water at room temperature taken as 1.333).

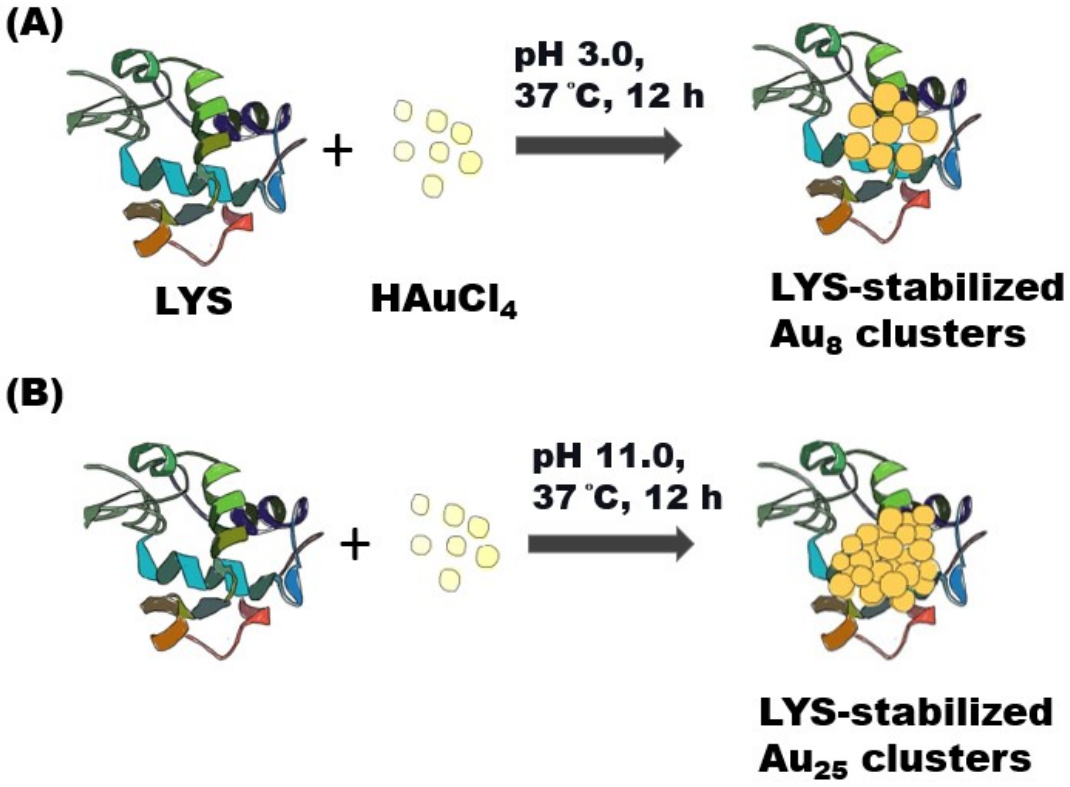

Figure S1. Schematic illustration associated with the preparation of (A) Lys-stabilized Au_8 clusters and (B) Lys-stabilized Au_{25} clusters. Both reactions were conducted at 37 °C in the dark and purified by dialysis (MWCO 1000 Da).

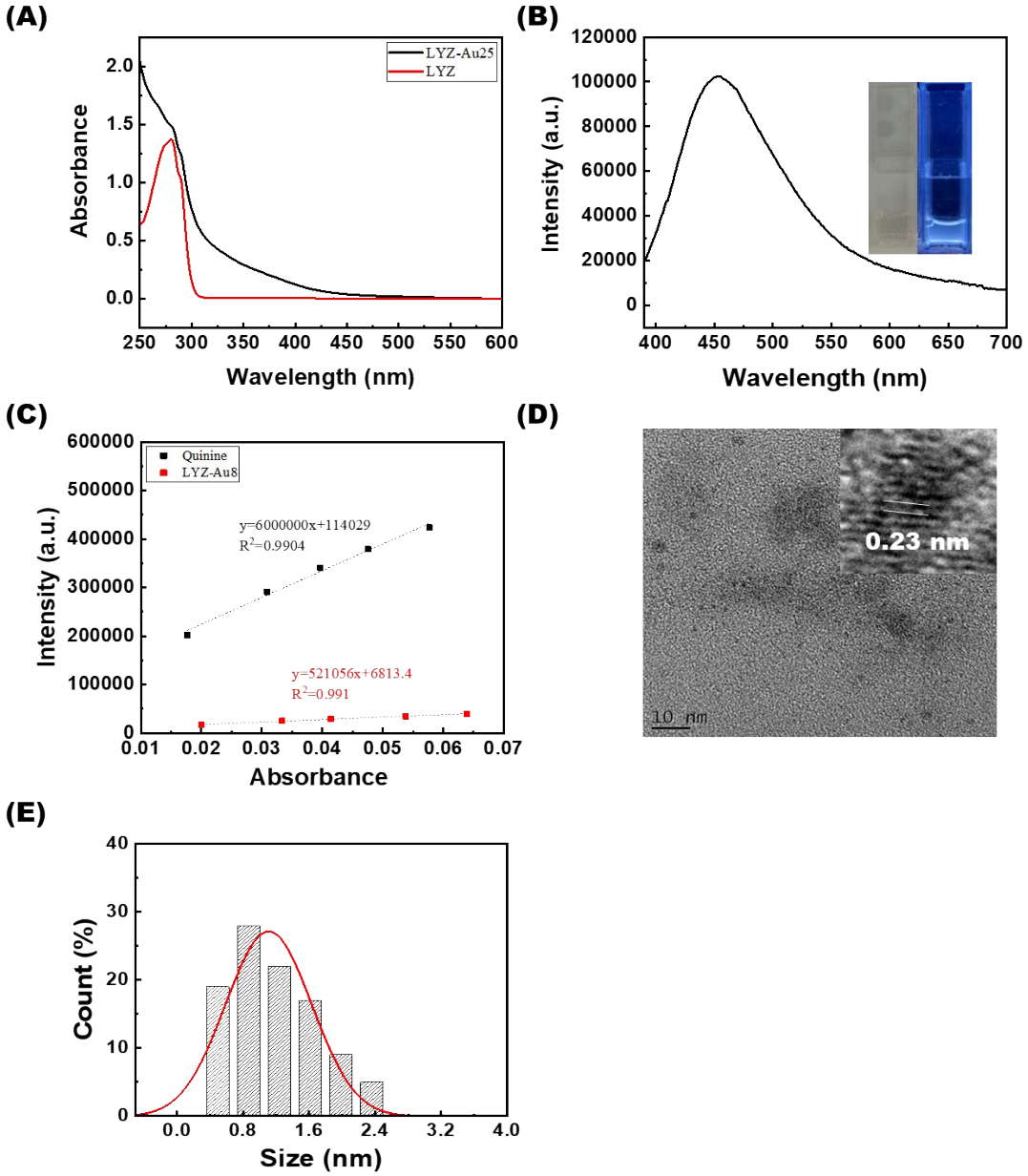

Figure S2. Optical and morphological characterization of LYZ-stabilized Au_8 clusters. (A) UV–vis absorption spectra of native LYZ (red) and LYZ-stabilized Au_8 clusters (black). (B) Photographs of LYZ-stabilized Au_8 clusters under daylight (left) and UV illumination (right) and their emission spectrum. (C) Plot of integrated emission intensity as a function of absorbance for the reference quinine sulfate (black) and the LYZ-stabilized Au_8 clusters (red). The slopes of the linear fits were used to calculate the QY. (D, E) TEM images and particle size distribution of Au_8 clusters (1.4 ± 0.5 nm, n = 100). The inset shows lattice fringes consistent with the Au(111) plane.

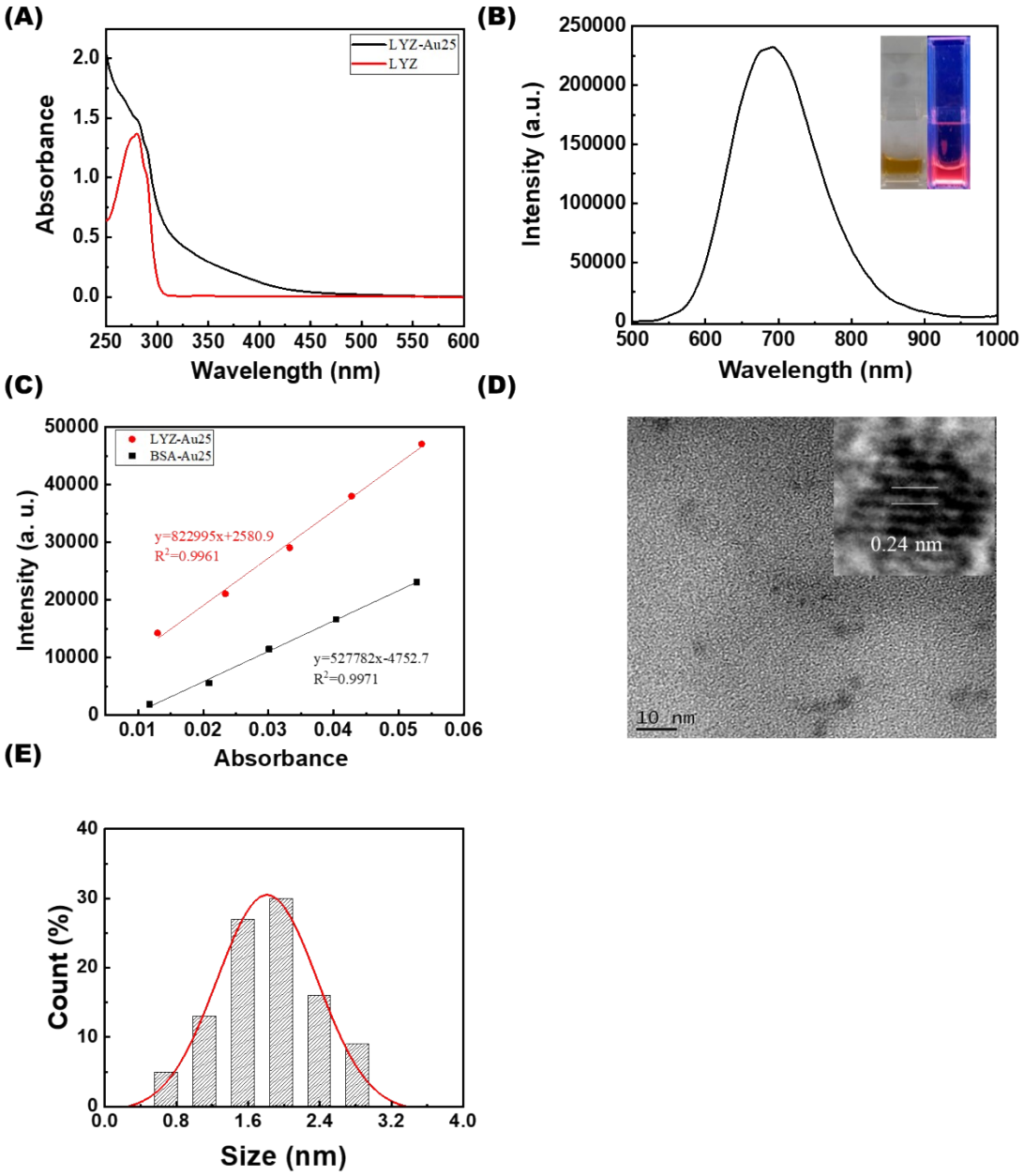

Figure S3. Optical and morphological characterization of LYZ-stabilized Au_{25} clusters. (A) UV–vis absorption spectra of native LYZ (red) and LYZ-stabilized Au_{25} clusters (black). (B) Photographs of LYZ-stabilized Au_{25} clusters under daylight (left) and UV illumination (right) and their emission spectrum. (C) Plot of integrated emission intensity as a function of absorbance for the reference BSA-stabilized Au_{25} clusters (black) and the LYZ-stabilized Au_{25} clusters (red). The slopes of the linear fits were used to calculate the QY. (D, E) TEM images and particle size distribution of Au_{25} clusters (1.5 ± 0.4 nm, n = 100). The inset shows lattice fringes consistent with the Au(111) plane.

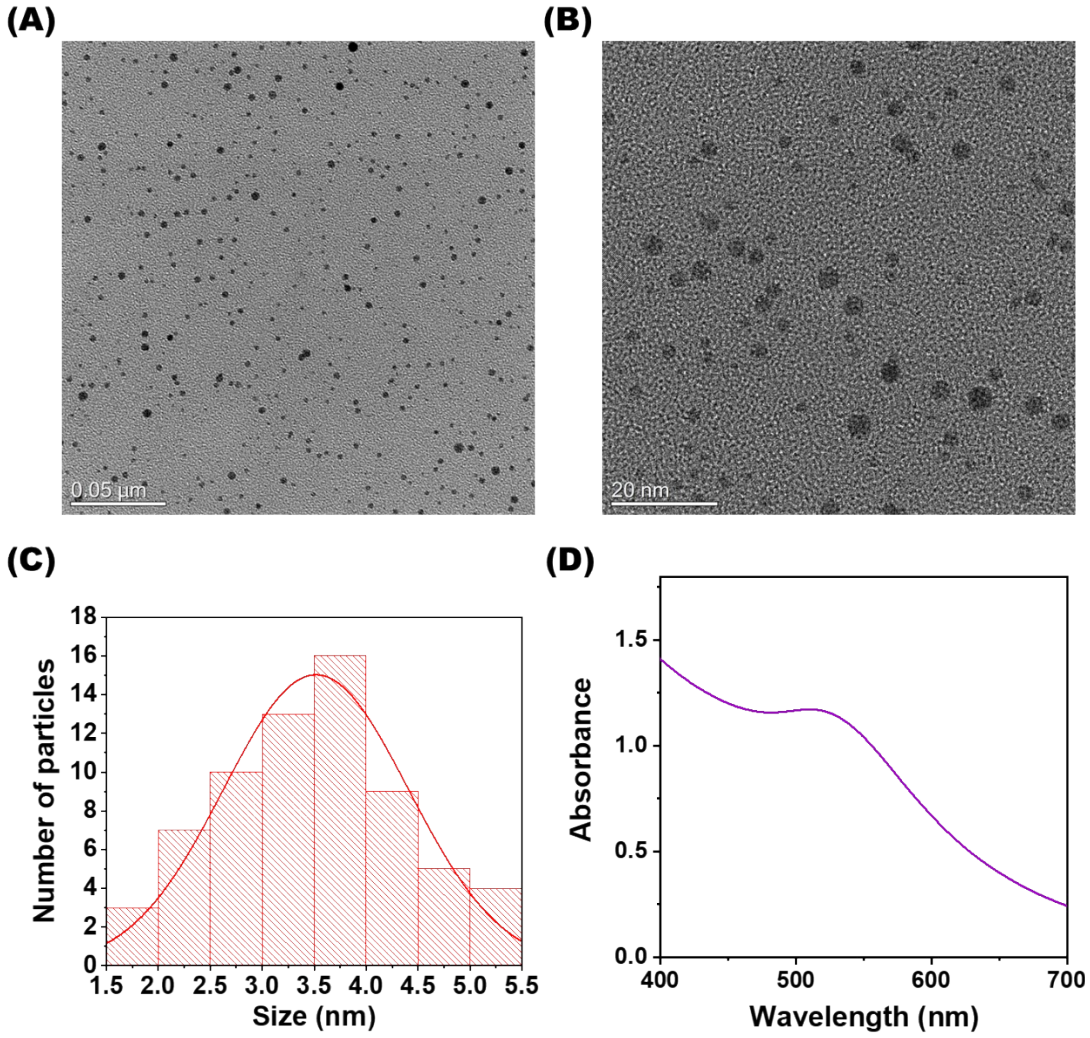

Figure S4. TEM characterization and optical signature of LYZ-stabilized AuNPs (~3.2 nm) clusters. (A, B) TEM images of AuNPs at different magnification. (C) Particle size distribution (3.2 ± 0.5 nm, n = 100) of LYZ-stabilized AuNPs (D) UV–vis absorption spectrum of LYZ-stabilized AuNPs.

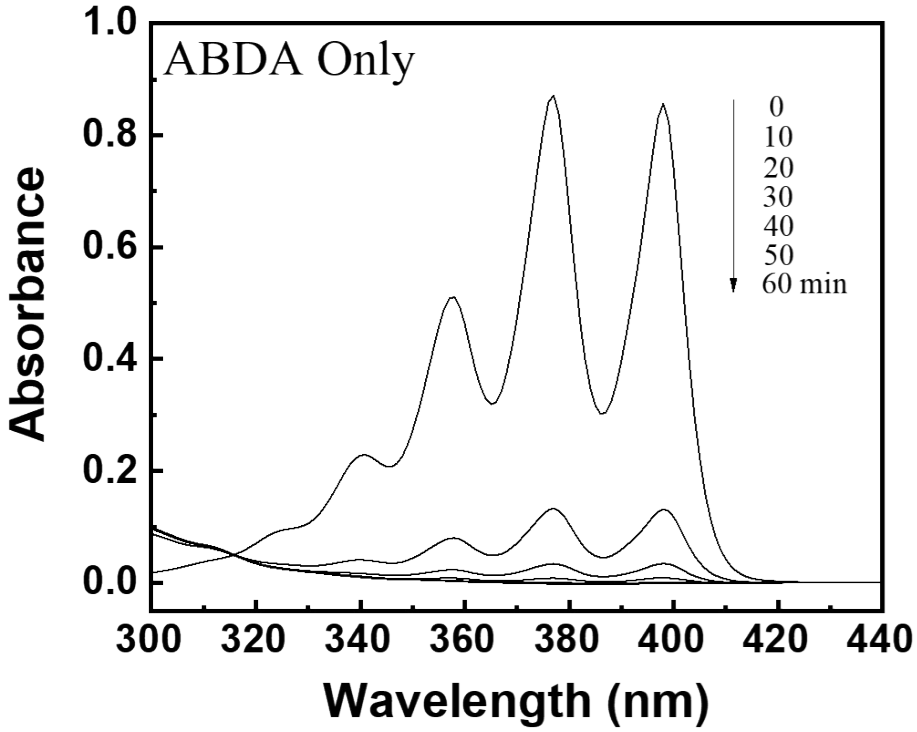

Figure S5. Time-dependent absorption spectra of ABDA-only solution under violet LED (400–420 nm).

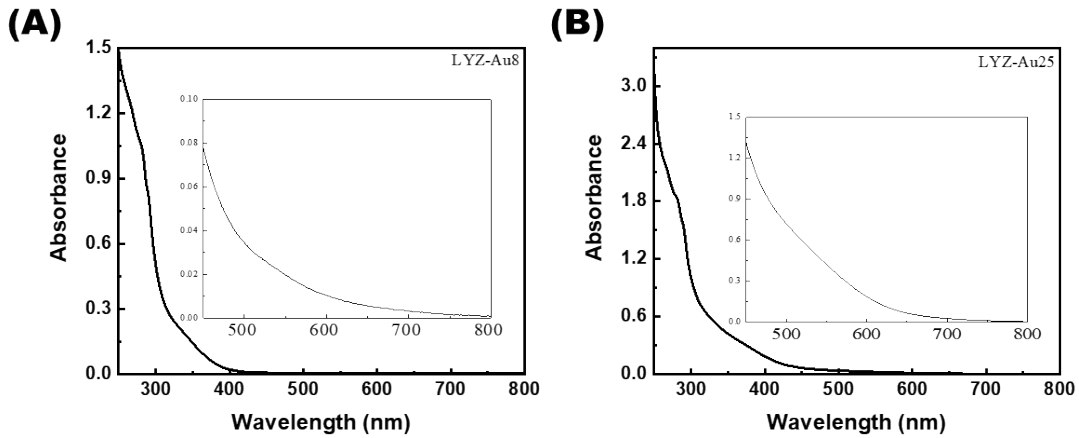

Figure S6. UV–vis absorption spectra of lysozyme-stabilized (A) Au_8 and (B) Au_{25} clusters. The main panel displays the full absorption profiles of both clusters, while the inset shows an enlarged view of the low-wavelength region to highlight the characteristic absorption features of Au_8 and Au_{25}.

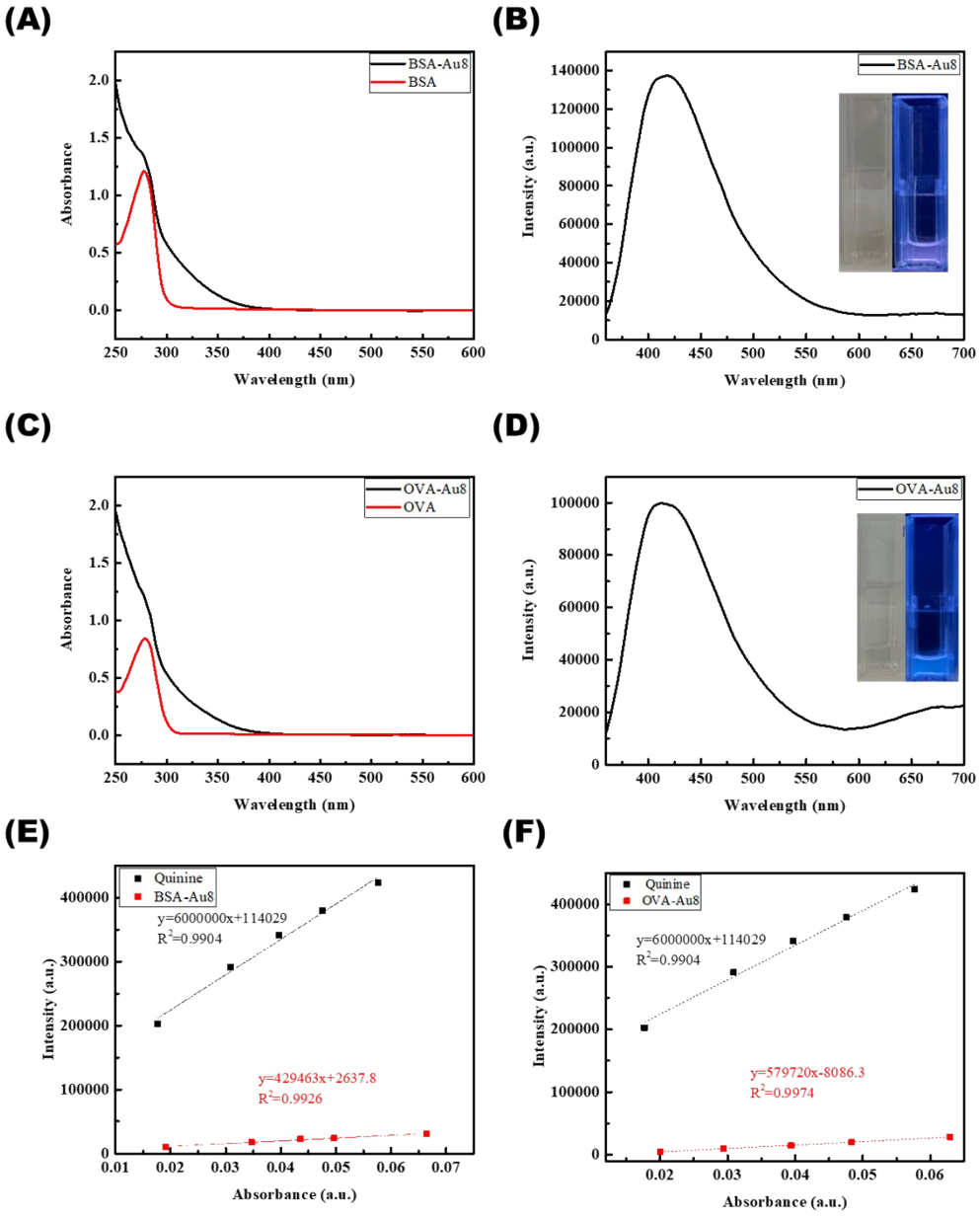

Figure S7. Optical features of BSA- and ovalbumin-stabilized Au_8 clusters. (A) UV–vis absorption spectra of native BSA (red) and BSA-stabilized Au_8 clusters (black). (B) Photographs of BSA-stabilized Au_8 clusters under daylight (left) and UV illumination (right) and their emission spectrum. (C) UV–vis absorption spectra of native ovalbumin (red) and ovalbumin-stabilized Au_8 clusters (black). (D) Photographs of ovalbumin-stabilized Au_8 clusters under daylight (left) and UV illumination (right) and their emission spectrum. (E, F) Plot of the absorbance versus integrated emission intensity for (E) BSA-stabilized Au_8 clusters (red) and reference quinine sulfate (black) and (F) ovalbumin-stabilized Au_8 clusters and reference quinine sulfate (black)

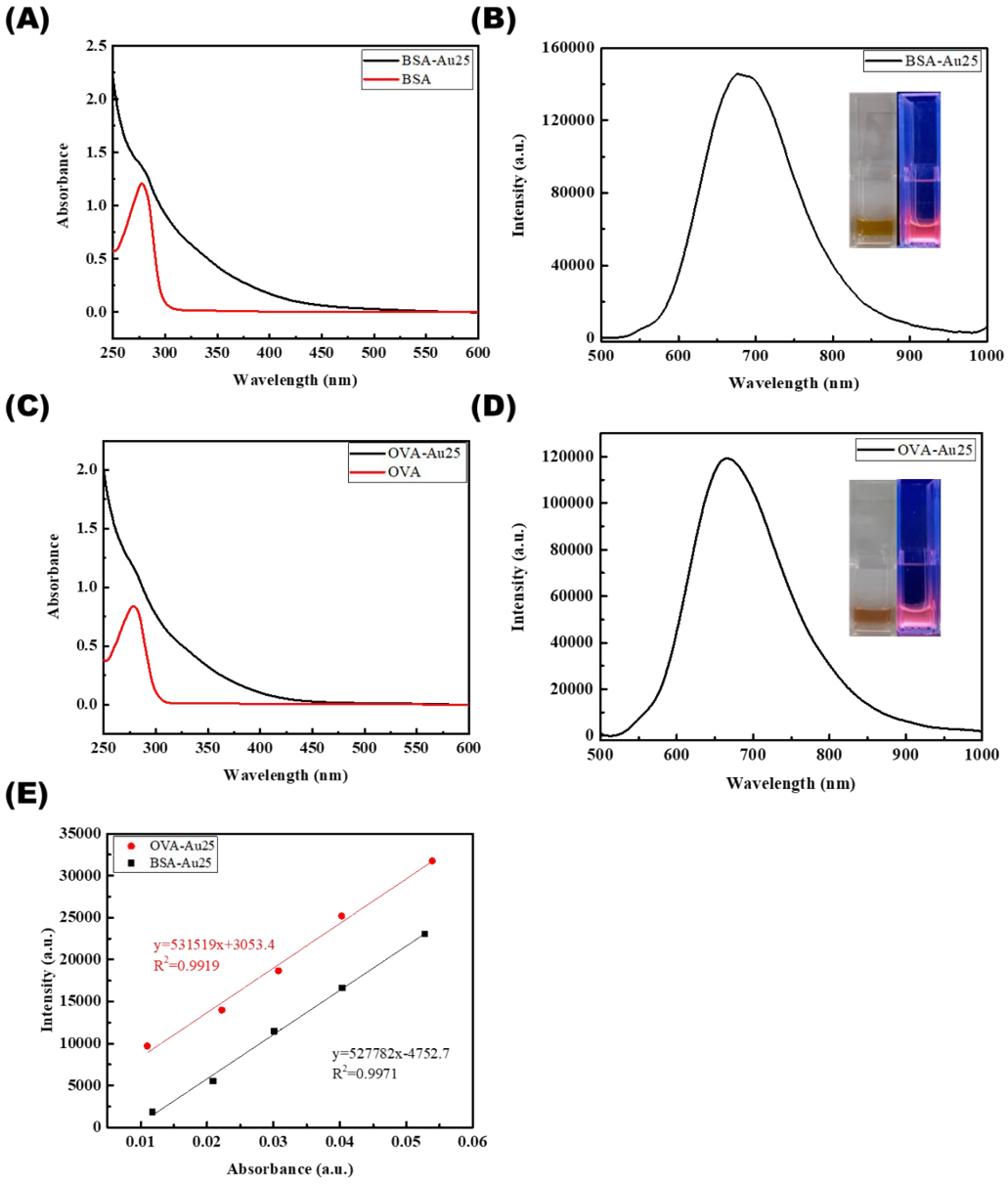

Figure S8. Optical features of BSA- and ovalbumin-stabilized Au_{25} clusters. (A) UV–vis absorption spectra of native BSA (red) and BSA-stabilized Au_{25} clusters (black). (B) Photographs of BSA-stabilized Au_{25} clusters under daylight (left) and UV illumination (right) and their emission spectrum. (C) UV–vis absorption spectra of native ovalbumin (red) and ovalbumin-stabilized Au_{25} clusters (black). (D) Photographs of ovalbumin-stabilized Au_{25} clusters under daylight (left) and UV illumination (right) and their emission spectrum. (E) Plot of the absorbance versus integrated emission intensity for reference BSA-stabilized Au_{25} clusters (black) and ovalbumin-stabilized Au_{25} clusters (red).

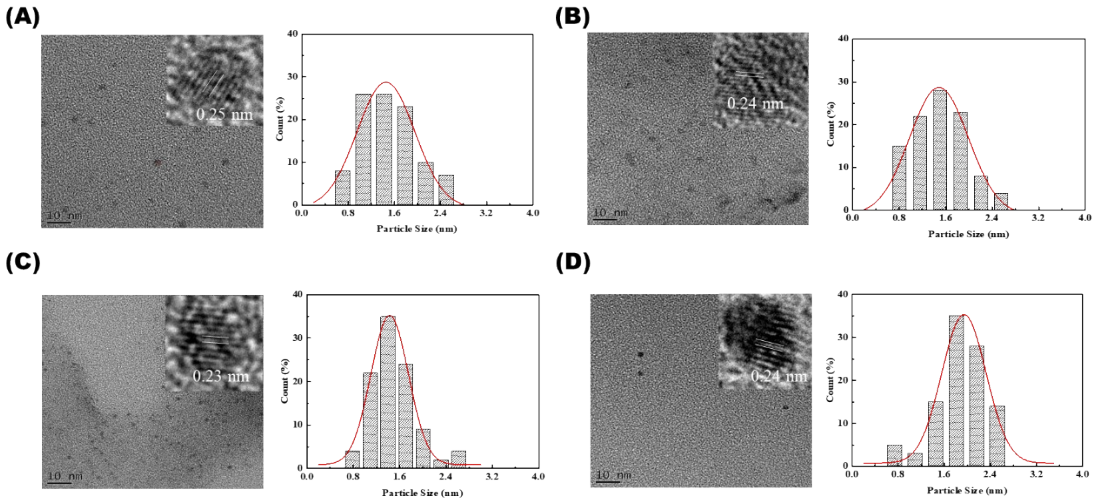

Figure S9. TEM images (left) and particle size distribution (right) of (A) BSA-stabilized Au_8 clusters, (B) ovalbumin-stabilized Au_8 clusters, (C) BSA-stabilized Au_{25} clusters, and (D) ovalbumin-stabilized Au_{25} clusters. (A–D) The inset shows lattice fringes consistent with the Au(111) plane.

Table S1. Properties and Literature of Au_8 clusters

Capping Ligands	**Excitation (nm)**	**Emission (nm)**	**XPS Au(0):Au(I)**	**How Determined to be Au_8 Clusters**	**Ref.**
Pepsin	330	480	Only Au(0) detected	MALDI-TOF MS; spherical Jellium model	*1*
Lysozyme Type VI	380	455	Only Au(0) detected	MALDI-TOF MS; spherical Jellium model	*2*
Dodecylamine & DMAET[a]	360	436	Not available	MALDI-TOF MS; optical spectroscopy	*3*
PAMAM Dendrimers (G4OH)	387	458	Not available	Spherical Jellium model; literature comparison	*4*
PAMAM Dendrimers (G4NH_2)	390	460	Not available	Spherical Jellium model;	*5*
DNase 1	395	460	Not available	Literature comparison	*6*
Polyethylenimine	353	445	Only Au(0) detected	ESI Mass Spectrometry; similarity to PAMAM-encapsulated Au_8	*7*
Bovine Serum Albumin	370	450	Only Au(0) detected	Spherical Jellium model; literature comparison	*8*
Human Hemoglobin	365	450	Do not specify an exact numerical ratio	Literature comparison	*9*
Peptide 1 & 3-MPA[b]	360	455	95 : 5	MALDI-TOF MS ; spherical Jellium model	*10*
MPT63 proteins	385	445	81:19	MALDI-TOF MS; spherical Jellium model	*11*

Gly20Cys/Gly40Cys Mutants[c]					
Lysozyme	370	454	Not detected	Spherical Jellium model; optical spectroscopy; literature comparison	*This work*
Ovalbumin	370	415	Not detected	Spherical Jellium model; optical spectroscopy; literature comparison	*This work*
Bovine serum albumin	370	429	Not detected	Spherical Jellium model; optical spectroscopy; literature comparison	*This work*

[a]2-(dimethylamino) ethanethiol; [b]3-mercaptopropionic acid; [c]A version of the protein where the glycine residues at position 20 and 40 have been replaced with cysteine.

Table S2. Properties and Literature of Au_{25} clusters

Capping Ligands	**Excitation (nm)**	**Emission (nm)**	**XPS Au(0):Au(I)**	**How Determined to be Au_8 Clusters**	**Ref.**
Pepsin	360	670	Only Au(0) detected	MALDI-TOF MS; spherical Jellium model	*1*
Lysozyme Type VI	380	635	Only Au(0) detected	MALDI-TOF MS; spherical Jellium model	*2*
glutathione (GSH) and 3-mercaptopropionic acid (MPA)	-	-	Only Au(0) detected	UV–vis and ESI-MS	*12*
Bovine serum albumin (BSA)	370; 530	685	Au(0) only	Spherical Jellium model; literature comparison MALDI-TOF MS; XPS measurements	*8*
BSA	470	640	Au(0) and Au(I)	MALDI-TOF MS; XPS measurements; literature comparison	*13*
Native bovine lactoferrin	445	650	Only Au(0) detected	MALDI-TOF-MS; XPS measurements	*14*
Captopril (Capt)	514	670		ESI-MS; MALDI-MS	*15*
DNase 1	460	640	Not available	Literature comparison	*6*
Sodium 3-(triphenylphosphonio)propane-1-thiolate bromide	488	670	Au(0) and Au(I)	ESI-TOF-MS	*16*
GSH, N-acetyl-l-	-	-	Not detected	ESI MS; literature comparison	*17*

cysteine (AcCys), Capt), and 4-mercapto benzoic acid					
Lysozyme	370	680-700	Not detected	Optical spectroscopy; literature comparison	*This work*
Ovalbumin	370	680-700	Not detected	Optical spectroscopy; literature comparison	*This work*
BSA	370	680-700	Not detected	Optical spectroscopy; literature comparison	*This work*

References

1. H. Kawasaki, K. Hamaguchi, I. Osaka and R. Arakawa, *Advanced Functional Materials*, 2011, **21**, 3508-3515.
2. T. H. Chen and W. L. Tseng, *Small*, 2012, **8**, 1912-1919.
3. W. Guo, J. Yuan and E. Wang, *Chemical Communications*, 2012, **48**, 3076-3078.
4. Y. Bao, C. Zhong, D. M. Vu, J. P. Temirov, R. B. Dyer and J. S. Martinez, *The Journal of Physical Chemistry C*, 2007, **111**, 12194-12198.
5. C.-P. Liu, T.-H. Wu, C.-Y. Liu, H.-J. Cheng and S.-Y. Lin, *Journal of Materials Chemistry B*, 2015, **3**, 191-197.
6. A. L. West, M. H. Griep, D. P. Cole and S. P. Karna, *Analytical chemistry*, 2014, **86**, 7377-7382.
7. H. Duan and S. Nie, *Journal of the American Chemical Society*, 2007, **129**, 2412-2413.
8. X. Le Guével, B. Hötzer, G. Jung, K. Hollemeyer, V. Trouillet and M. Schneider, *The Journal of Physical Chemistry C*, 2011, **115**, 10955-10963.
9. M. Shamsipur, F. Molaabasi, M. Shanehsaz and A. A. Moosavi-Movahedi, *Microchimica Acta*, 2015, **182**, 1131-1141.
10. Q. Wen, Y. Gu, L.-J. Tang, R.-Q. Yu and J.-H. Jiang, *Analytical chemistry*, 2013, **85**, 11681-11685.
11. S. Chall, S. S. Mati, I. Das, A. Kundu, G. De and K. Chattopadhyay, *Langmuir*, 2017, **33**, 12120-12129.
12. Y. Yu, X. Chen, Q. Yao, Y. Yu, N. Yan and J. Xie, *Chemistry of Materials*, 2013, **25**, 946-952.
13. J. Xie, Y. Zheng and J. Y. Ying, *Journal of the American Chemical Society*, 2009, **131**, 888-889.

14. P. L. Xavier, K. Chaudhari, P. K. Verma, S. K. Pal and T. Pradeep, *Nanoscale*, 2010, **2**, 2769-2776.
15. S. Kumar and R. Jin, *Nanoscale*, 2012, **4**, 4222-4227.
16. Y. Hua, Z.-H. Shao, A. Zhai, L.-J. Zhang, Z.-Y. Wang, G. Zhao, F. Xie, J.-Q. Liu, X. Zhao and X. Chen, *ACS nano*, 2023, **17**, 7837-7846.
17. S. Kundu, H. Yuan and R. Antoine, *The Journal of Physical Chemistry Letters*, 2025, **16**, 8480-8485.